A Probabilistic Approach to Liquid Level Detection in Cups Using an RGB-D Camera

Chau Do Tobias Schubert Wolfram Burgard

***Abstract*— Robotic assistants have the potential to greatly improve our quality of life by supporting us in our daily activities. A service robot acting autonomously in an indoor environment is faced with very complex tasks. Consider the problem of pouring a liquid into a cup, the robot should first determine if the cup is empty or partially filled. RGB-D cameras provide noisy depth measurements which depend on the opaqueness and refraction index of the liquid. In this paper, we present a novel probabilistic approach for estimating the fill-level of a liquid in a cup using an RGB-D camera. Our approach does not make any assumptions about the properties of the liquid like its opaqueness or its refraction index. We develop a probabilistic model using features extracted from RGB and depth data. Our experiments demonstrate the robustness of our method and an improvement over the state of the art.**

I. INTRODUCTION

Autonomous behavior is necessary for domestic service robots to be effective in their roles. One area in which they may aid us is the preparation and serving of beverages. In general dealing with liquids is difficult due to their varying characteristics and the overwhelming selection available. However, there are many situations where a domestic service robot will encounter different liquids making the correct perception of the liquid's properties a necessary skill. In this paper, we consider the challenging problem of estimating the fill level of a cup filled with an unknown liquid using an RGB-D camera.

The problem of estimating the fill-level of a liquid is complicated by the fact that not all liquids behave the same way when viewed with an RGB-D camera. Depth image cameras, like the Microsoft Kinect v1 (abbr. Kinect) and ASUS Xtion PRO LIVE (abbr. Xtion), send a pattern of infrared light to the surroundings and compare the returned pattern to a saved one for depth detection. Due to the refraction of light on the liquid boundary by transparent liquids, the computed depth values of the liquid height do not represent the real value. For example a full cup of water appears a third full if one only looks at the point cloud data of the liquid level directly. This effect can be seen in Fig. 1. Opaque liquids on the other hand reflect most of the light resulting in a reliable liquid height in the point cloud.

In this paper we present a novel probabilistic approach to determine the fill-level of the liquid in a cup using an RGB-D camera. Our approach uses several point clouds and images obtained from a cup filled with a liquid taken from different viewing angles. Based on these observations, it is able to determine as to whether the liquid is opaque or transparent, and what the height of the liquid in the cup is. To achieve robust estimates, it also determines an approximate index of refraction for clear liquids.

*This work has been partly supported by BrainLinks-BrainTools, Cluster of Excellence funded by the German Research Foundation (DFG, grant number EXC 1086), the German Federal Ministry of Education Research grants 16SV5834 NASS, 0316064C BrainCon, and grant BMI-Bot by the Baden-Württemberg Stiftung.

All authors are with the Department of Computer Science at the University of Freiburg, Georges-Köhler-Allee 79, 79110 Freiburg, Germany

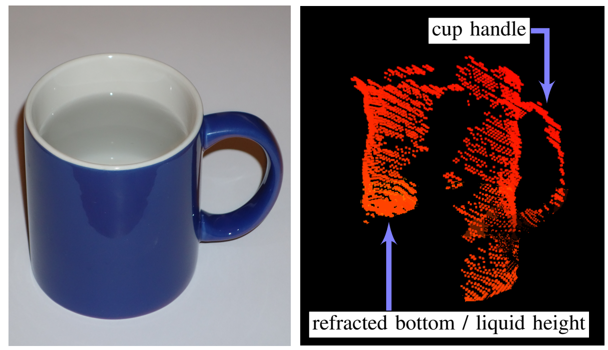

(a) Cup filled with water (b) Point cloud of the cup

Fig. 1. Example output from an Xtion showing the different views between image and point cloud. Figure (a) shows the cup filled with water 2 cm from the rim. Figure (b) shows the corresponding point cloud of the cup with a refracted bottom that is significantly lower than the water level

II. RELATED WORK

The limitations of RGB-D cameras, such as the Kinect and Xtion, for detecting transparent objects are well known. Wang et al. [14] combine RGB data and depth data to localize glass objects in an environment. They do so based on the refraction and attenuation of a signal passing through the glass object. Lysenkov et al. [10] use an RGB-D camera to detect the pose of rigid transparent objects. Using a time-of-flight camera, Klank et al. [9], provide an approach to detect transparent objects based on their absorption of light in certain wavelengths. These papers do not consider liquids, let alone the detection of liquid height.

The problem of detecting the height of a liquid is also present in other areas outside of the domestic environment. In particular, Pithadiya et al. [12] looked at different edge detection algorithms for detecting whether or not water bottles are over or under filled. However, instead of determining the actual liquid height, the detected edges are compared to a reference line to determine this.

For the restaurant industry, Bhattacharyya et al. [2], use RFID tags for liquid level detection in beverage glasses and liquor bottles. Dietz et al. [4] use specially designed glasses and a coil embedded into a table which provides power and data exchange with the glasses. Gellersen et al. [7] use augmented coffee cups that are able to sense and communicate. All of these papers require sensors or tags attached to the glasses or cups. In contrast, our approach requires only an RGB-D sensor.

Elbrechter et al. [5] estimate the viscosity of different liquids used in food preparation. They collect information on surface changes of a liquid resulting from a pushing motion and use this to train a classifier. Chitta et al. [3] use tactile information obtained by manipulating a bottle or can to determine if they are open or closed and full or empty. They do not consider the detection of the liquid height.

Morris and Kutulakos [11] use stereo cameras to reconstruct a refractive surface. To do this, patterns are placed underneath the liquid surface. This differs from our focus on cups which typically do not have a pattern on the bottom.

Most relevant to our work, Hara et al. [8] investigated the measurement of opaque and transparent liquids using an RGB-D camera. They determined a relationship between the height measured in the depth data and the actual height of the liquid. However, they were unable to determine the index of refraction of the liquid from the depth data and they could not distinguish between a transparent and opaque liquid. These are crucial aspects in correctly processing the data from an RGB-D sensor. As a result, they were only able to detect the presence of a liquid in the cup by checking if the height in the point cloud is higher than the height of the cup bottom.

The main contribution of this paper is the probabilistic formulation of the liquid fill-level detection. Furthermore, in contrast to Hara et al. [8], we are able to handle both opaque and transparent liquids and do not require the knowledge of the index of refraction beforehand.

III. Probabilistic Approach for Fill Level Estimation

Our main goal is to detect the liquid height h out of RGB data D_{rgb} and depth data D_d. Since we deal with low cost RGB-D cameras such as the Kinect and Xtion, considerable noise is present in these observations. We use a probabilistic formulation to take the resulting uncertainty into account. Thus, our goal is to find the most probable height value h given the data D_{rgb} and D_d. In other words we want to solve the optimization problem

$$\arg\max_{h} \; p(h \mid D_{rgb}, D_d). \tag{1}$$

We present two features, D_{h_e} and D_{h_r}, which we extract from D_{rgb} and D_d and which are relevant for robustly estimating the liquid height. For the RGB data, D_{rgb}, we apply an edge detection algorithm to extract the edge between the liquid and the cup. The corresponding depth data, D_d, is then used to associate the detected edge points with height values. We denote the height values we obtain by the edge detection as D_{h_e}. In addition, we extract the raw height values, D_{h_r}, and viewing angles, D_α, from the depth data D_d (see Fig. 3). With the help of Snell's law the liquid height can then be computed. The whole optimization problem then reads

$$\arg\max_{h} \; p(h \mid D_{rgb}, D_d) = \arg\max_{h} \; p(h \mid D_{h_e}, D_{h_r}, D_\alpha). \tag{2}$$

With Bayes' theorem we obtain

$$p(h \mid D_{h_e}, D_{h_r}, D_\alpha) = \frac{p(D_{h_e}, D_{h_r} \mid h, D_\alpha) p(h \mid D_\alpha)}{p(D_{h_e}, D_{h_r} \mid D_\alpha)}. \tag{3}$$

Due to a lack of prior knowledge we assume the probability $p(h \mid D_\alpha)$ to be uniformly distributed in the range of possible height values, i.e., $p(h \mid D_\alpha) = \mathcal{U}([0, h_C])(h)$, where 0 is the inner cup bottom and h_C is the height of the cup. Next, we assume the two methods to be independent, i.e.,

$$p(D_{h_e}, D_{h_r} \mid h, D_\alpha) = p(D_{h_e} \mid h, D_\alpha) \cdot p(D_{h_r} \mid h, D_\alpha). \tag{4}$$

Summarizing, we have to solve the optimization problem

$$\arg\max_{h \in [0, h_C]} \; p(D_{h_e} \mid h, D_\alpha) \cdot p(D_{h_r} \mid h, D_\alpha). \tag{5}$$

We also look at each model individually in order to compare them to the combined model. In the following sections, we will describe how the two probabilistic models are defined.

A. Probabilistic Model for the RGB Data

In this section, we focus on the term $p(D_{h_e} \mid h, D_\alpha)$. The liquid height in a cup is detected using the image and point cloud from the RGB-D camera taken at approximately the same point in time. Transparent liquids such as water are more problematic since it is difficult to distinguish between cup and liquid. A salient feature that is common for different liquid and cup combinations is the edge that is formed where liquid meets cup. The idea is to employ an edge detection algorithm to determine the height of the liquid.

To keep the approach as general as possible, we locate the cup by detecting a cylinder in the point cloud using RANSAC [6]. Next, we determine a circular model of the rim of the cup and project it into the image. This determines the area used for the image processing steps. Fig. 2(a) shows the detected cup rim projected on the image. Next we apply an edge detection algorithm to the grayscale converted image to find the edge between the liquid and cup. We use the Scharr operator for this purpose, as it turned out to yield robust edge detection results. To mitigate the affects of lighting conditions (e.g., false edge detection due to reflections), data was collected for various lighting conditions and view angles.

Next, we generate theoretical liquid height edges in the image dependent on the height of the cup. This was done by detecting the cup height and dividing this height into steps. A circle was generated at each step and projected into the image. In order to estimate the liquid height, we determine which generated edge is closest to the detected edge. Fig. 2(b) shows the detected edge of the liquid in red and a few of the generated theoretical liquid height edges.

Due to variation in illumination, false edge detections occur and an accurate liquid height may not be detected using only one image-point cloud pair. In our experiments we observed that mainly three different cases are detected.

Besides the true edge between the liquid and the cup, a shadow caused by the tapering of the inside of the cup (this was present in all the cups we checked) is detected a few millimeters below the cup rim. In the case of transparent liquids, like water and vodka, the cup bottom edge is detected as well. Due to the refraction of light, the height of the detected cup bottom seen in the RGB images (denoted with h_{cb}) depends on the viewing angle α and the true liquid height h. We model this by introducing two hidden variables E and V, where E stands for edge and takes the values $\{th, cr, cb\} = \{\text{true height, cup rim, cup bottom}\}$, and V stands for the visibility of the bottom and takes the values $\{v, nv\} = \{\text{visible, not visible}\}$. Thus, we can model the height h_e given by the edge detection through

$$h_e = \begin{cases} h + \nu_{th} & \text{if} \quad E = th \\ h_{cr} + \nu_{cr} & \text{if} \quad E = cr \\ h_{cb}(h, \alpha) + \nu_{cb} & \text{if} \quad E = cb \text{ \& } V = v \end{cases}, \tag{6}$$

where h_{cr} denotes the height of the shadow and $\nu_{th(cr,cb)}$ denotes Gaussian noise with zero mean. We collect a set of height values $D_{h_e} = \{h_{e,i}\}_{i=1}^{N}$ and corresponding viewing angles $D_\alpha = \{\alpha_i\}_{i=1}^{N}$ using the RGB-D sensor. Under the assumption that these data points are independent, we obtain

$$p(D_{h_e} \mid h, D_\alpha) = \prod_{i=1}^{N} p\left(h_{e,i} \mid h, \alpha_i\right). \tag{7}$$

According to Eq. (6) and by marginalizing over the hidden variables E and V, the probability to obtain the height $h_{e,i}$ given the true height value $h = h_{th}$ and the viewing angle α_i is given by a mixture of Gaussians

$$p\left(h_{e,i} \mid h, \alpha_i\right) = \sum_{\substack{x \in \{th, cr, cb\} \\ y \in \{v, nv\}}} p(E = x, V = y) \cdot \mathcal{N}(h_e; h_x, \nu_x),$$

where we assume the edge case (E, V) to be independent of the tuple (h, α_i), i.e., $p(E, V \mid h, \alpha_i) = p(E, V)$ and we use $p(E = cb, V = nv) = 0$. Thus, the probability $p\left(h_e \mid h, \alpha\right)$ is given by a mixture of up to three Gaussians.

We use a training dataset to compute the parameters of the mixture of Gaussians and we employ the Bayesian information criterion (BIC) [13] to jointly find the optimal fit for the training dataset with a minimal number of Gaussians. In Section IV we refer to this model as the RGB model and optimize it for comparison.

B. Probabilistic Model for Depth Data

Hara et al. [8] showed that given the refraction index of the transparent liquid and the measured liquid height from the point cloud, one can compute the real liquid height using Snell's law. The drawbacks of this method are that it is not applicable to opaque liquids and that for clear liquids the refraction index must be known beforehand.

The Kinect and the Xtion sensors consist of an infrared projector that illuminates the scene with a speckle pattern and an infrared camera that detects the pattern. These two parts are separated by 75 mm, referred to as baseline b. The depth is computed using triangulation. In Fig. 3 we illustrate the scenario for liquid detection. The light beam is refracted on the liquid surface to a reflection point R on the cup bottom. It is then reflected from the cup bottom and again refracted at the liquid surface and is captured by the infrared camera. We can thus measure the point M using triangulation. Due to the refraction on the liquid surface the measured point differs from the actual reflection point. It was shown by Hara et al. [8] that in the case where the reflection point R is on the perpendicular bisector of the baseline b, the projected beam and the received beam intersect. In the case the reflection point R is not on the perpendicular bisector, the beams are skewed and an intersection point does not exist. Hara et al. [8] also demonstrated that this effect is rather negligible. We design our experiments in such a way, that the reflection point R lies close to the perpendicular bisector. In this case one can assume that the angle α and β in Fig. 3 are equal. Given the measured point M we can then compute the liquid level perceived by the RGB-D camera $h_r = \|M - R\|$, which stands for raw height and is measured from the point cloud. We determine the liquid height h from the index of refraction n, the angle α and the raw height h_r. Given this arrangement, we describe the liquid height h with respect to the measured liquid height, h_r and the index of refraction by

$$h = h_r + h_d = \frac{\tan(\alpha)}{\tan(\alpha_l)} h_d, \tag{8}$$

where α_l denotes the angle of the refracted light beam and h_d is defined by the first equality. Given the true liquid height,

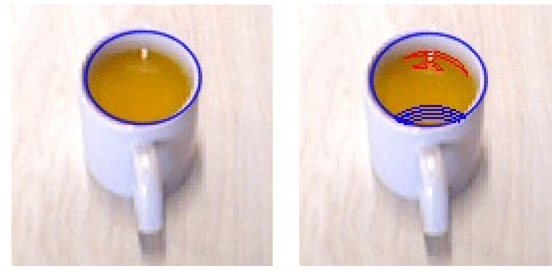

(a) Cup rim (b) Liquid contour (red)

Fig. 2. Example of the RGB feature extraction. Figure (a) shows the rim of the cup detected in the point cloud and projected into the image. In figure (b) the red contour is the detected edge for the liquid and the blue contours represent the theoretical liquid height edges for lower liquid levels

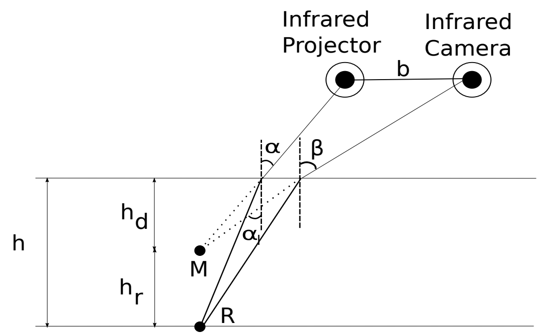

Fig. 3. Detection of liquid by a depth camera based on triangulation with refraction of the infrared light

we comput the raw measured height h_r according to

$$h_r = \left(1 - \frac{\tan(\alpha_l)}{\tan(\alpha)}\right) h. \tag{9}$$

The value for $\tan(\alpha_l)$ can be described in terms of α and the index of refraction for the liquid (n_l) through Snell's law

$$\tan(\alpha_l) = \frac{\sin(\alpha)}{\sqrt{n_l^2 - \sin^2(\alpha)}} = \frac{\cos(\alpha)}{\sqrt{n_l^2 - 1 + \cos^2(\alpha)}} \tan(\alpha). \tag{10}$$

Substituting Eq. (10) into Eq. (9) results in

$$h_r = \left(1 - \frac{\cos(\alpha)}{\sqrt{n_l^2 - 1 + \cos^2(\alpha)}}\right) h := f(\cos(\alpha); n_l, h). \tag{11}$$

In practice, measuring the angle and the raw height exactly is difficult, since there is typically a lot of noise. For example, it can be introduced by the unevenness of the surfaces such as the cup bottom, which affects the reflection of the light. Furthermore, there is inherent noise in the point clouds captured by the RGB-D camera. The depth resolution of the Kinect and Xtion varies from a few millimeters in the near range (50 cm) to a resolution of about 20 cm in the far range (8 m), see Andersen et al. [1]. Taking the noise into account we reformulate Eq. (11) as

$$h_r = f(\cos(\alpha) + \nu_\alpha; n_l, h) + \nu_r, \tag{12}$$

where ν_r, ν_α denote noise terms for the raw height h_r and angle α respectively, and f corresponds to

$$f(x; y, z) = \left(1 - \frac{x}{\sqrt{y^2 - 1 + x^2}}\right) z.$$

We assume the noise ν_r and the noise ν_α to be normally distributed, with zero mean and covariances σ_r and σ_α respectively. We approximate Eq. (12) with help of the first order Taylor expansion along the dimension x and obtain

$$h_r = f(\cos(\alpha); n_l, h) + \nabla_x f(\cos(\alpha); n_l, h)\nu_\alpha + \nu_r. \tag{13}$$

The right hand side $\nabla_x f(\cos(\alpha); n_l, h)\nu_\alpha + \nu_r$ is normally distributed with zero mean and the variance is given by $\sigma = \sigma(n_l) := \left(\nabla_x f(\cos(\alpha); n_l, h)\right)^2 \sigma_\alpha + \sigma_r$, where

$$\nabla_x f(x; y, z) = \frac{\left(1 - y^2\right) z}{\left(y^2 - 1 + x^2\right)^{\frac{3}{2}}}.$$

In our experiments we observed that opaque liquids do not act like refractive liquids for the Kinect and Xtion but instead as non-refractive material ($n_l = \infty$). We model this behavior by introducing the binary hidden variable T, which stands for transmittance, and takes the values $\{\mathrm{op}, \mathrm{cl}\} = \{\mathrm{opaque}, \mathrm{clear}\}$. In the case of opaque liquids Eq. (12) reads as

$$h_r = h + \nu_r. \tag{14}$$

Given these state equations, we are now able to model $p(D_{h_r} \mid h, D_\alpha)$. First of all, we assume the data points to be independent, giving

$$p(D_{h_r} \mid h, D_\alpha) = \prod_{i=1}^{N} p\left(h_{r,i} \mid h, \alpha_i\right). \tag{15}$$

Since the transmittance T of the liquid is not known beforehand, we marginalize over this hidden variable and obtain

$$p\left(h_{r,i} \mid h, \alpha_i\right) = \sum_{x \in \{op, cl\}} p\left(h_{r,i} \mid h, \alpha_i, T = x\right) p(T = x), \tag{16}$$

where we assume independence between the tuple (h, α_i) and the transmittance, i.e., $p(T = x \mid h, \alpha_i) = p(T = x)$. We marginalize over the index of refraction n_l and obtain

$$\begin{aligned} &p\left(h_{r,i} \mid h, \alpha_i, T\right) \\ &= \left[\int p\left(h_{r,i} \mid n_l, h, \alpha_i, T\right) dP\left(n_l \mid h, \alpha_i, T\right)\right]. \end{aligned} \tag{17}$$

In the case of clear liquids we assume its refractive index to lie in the range of $[n_L, n_H]$. In the experiments we chose $[1.33, 1.47]$, which is not a substantial restriction since most household liquids fall in this range. Furthermore, we assume the refractive index to be uniformly distributed, i.e.,

$$dP\left(n_l \mid h, \alpha_i, T = cl\right) = \mathcal{U}(n_L, n_H)(n_l). \tag{18}$$

As mentioned above, opaque liquids act like non-refractive solids ($n_l = \infty$), which can be modeled by a delta distribution

$$dP\left(n_l \mid h, \alpha_i, T = op\right) = \delta_\infty(n_l). \tag{19}$$

With help of Eq. (12) and Eq. (13), we obtain

$$p\left(h_{r,i} \,|\, h, \alpha_i, T{=}cl\right) = \fint_{n_L}^{n_H} \mathcal{N}\left(h_{r,i}; f(\cos(\alpha_i); n_l, h), \sigma\right) dn_l,$$

$$p\left(h_{r,i} \,|\, h, \alpha_i, T{=}op\right) = \mathcal{N}\left(h_{r,i}; h, \sigma_r\right).$$

Summarizing, the probability $p(D_{h_r} \mid h, D_\alpha)$ is equal to

$$\begin{aligned} \prod_{i=1}^{N} \Big[&p(T = cl) \cdot \fint_{n_L}^{n_H} \mathcal{N}\left(h_{r,i}; f(\cos(\alpha_i); n_l, h), \sigma\right)\ dn_l \\ &+ p(T = op) \cdot \mathcal{N}\left(h_{r,i}; h, \sigma_r\right) \Big]. \end{aligned} \tag{20}$$

One might also be interested in finding the refraction index and transmittance of the liquid. To avoid clutter in the equations, we combine both variables in a variable r, which stands for refractiveness. Thereby, in the case of a clear liquid, r is equal to the refraction index n and in the case of an opaque liquid it is equal to ∞. We use the following approximation

$$p(D_{h_r} \mid h, D_\alpha) \approx \operatorname*{arg\,max}_{r \in [n_L, n_H] \cup \{\infty\}} p(D_{h_r} \mid h, r, D_\alpha). \tag{21}$$

In addition to the optimization problem of Eq. (5), we optimize this individual model for comparison in Section IV, where this model is referred to as DEPTH. Based on the approximation given in Eq. (21) we obtain the optimization problem

$$\underset{\substack{h\in[0,h_C]\\ r\in[n_L,n_H]\cup\{\infty\}}}{\arg\max} \prod_{i=1}^{N} \mathcal{N}\left(h_{r,i}; f(\cos(\alpha_i); r, h), \sigma\right). \quad (22)$$

We can write the equation in closed form due to the limits $\lim_{y\to\infty} f(x; y, z) = z$ and $\lim_{y\to\infty} \sigma(y) = \sigma_r$. We are interested in solving this optimization problem in order to find the index of refraction of the liquid.

IV. Experiments

We restricted the liquids tested to the following: water, vodka, oil, cola, apple juice, orange juice and milk. These liquids are common in a household and represent the varying properties of liquids that make height detection so difficult. Vodka is visually the same as water but has a different index of refraction and olive oil has a more distinct index of refraction from water. Milk and orange juice are opaque liquids, mainly reflecting the infrared pattern off the surface. This implies that the height measured in the point cloud accurately represents the actual height of the liquid. Cola on the other hand, appears opaque in the images, but behaves like a transparent liquid in the point cloud. Like water, vodka and apple juice, it refracts the infrared pattern.

We used two typical coffee mugs in our experiments, but our methods can easily be extended to other kinds of cups. To make the experiments more manageable, we collected data for a fixed set of liquid heights defined as a fraction of the fullness of the cup. For the cups that we used, we defined a full cup as a liquid height 2 cm from the rim. In addition to the full level, we collected data at one-quarter full, one-half full and three-quarters full, which were determined based on the full height value. We collected two different datasets. For dataset one, we used a fixed construction, along which the camera was moved. This resulted in accurate depth estimations. For this dataset, the lighting conditions were suboptimal, reducing the effectiveness of the RGB method. Dataset two was collected through moving the camera by hand. The depth measurements were not as good as with the fixed construction. However, the light conditions were improved resulting in better edge detection. At each height for each liquid, there were 12 runs recorded for dataset one and 10 runs for dataset two. Each run contained around 50 image-point cloud pairs.

1) Liquid Level Estimation: We compare our joint model based on Eq. (5) for liquid level estimation and refer to it as RGB_DEPTH. Our joint model combines two individual probabilistic models which we use as a comparison to emphasize the advantage of using a joint model. As mentioned before, these are referred to as RGB (see Eq. (7)) and DEPTH (see Eq. (20)). We compare our models with that of Hara et al. [8] in which we assume the index of refraction to be that of water, i.e., 1.33, since it is not possible to determine the index of refraction using their method. This is referred to as HARA14 in the tables. Furthermore we compare with a naive approach assuming that the point cloud height is correct (i.e., just using h_r). This is denoted as RAW.

Table I shows the total and percentage errors of the estimated heights to the ground truth. We take the mean and standard deviation over all liquids and filling levels. Overall the combined model outperforms the state of the art.

TABLE I

Fluid Level Error

	Dataset one	
Method	$\mu \pm \sigma$ [mm]	$\mu \pm \sigma$ [%]
RGB_DEPTH:	3.1 ± 4.1	6.7 ± 10.0
RGB:	9.0 ± 11.2	18.6 ± 24.6
DEPTH:	4.0 ± 5.0	9.7 ± 16.1
HARA14:	10.9 ± 11.9	25.6 ± 33.3
RAW:	25.2 ± 18.4	46.6 ± 29.6
	Dataset two	
Method	$\mu \pm \sigma$ [mm]	$\mu \pm \sigma$ [%]
RGB_DEPTH:	7.6 ± 13.2	33.6 ± 68.8
RGB:	10.6 ± 17.4	32.8 ± 61.5
DEPTH:	8.3 ± 12.4	35.8 ± 66.3
HARA14:	19.0 ± 16.1	64.0 ± 75.8
RAW:	17.0 ± 17.4	39.7 ± 34.0

The fluid level estimation differs between the individual liquids and fill levels. In Table II we show the errors, in percentage of the full cup level, from the estimated height values for all liquids and height levels from both datasets we collected. As mentioned above, the method from Hara et al. [8] is not able to detect if the liquid is opaque or not, which explains the large differences for the opaque liquids. In contrast to the work of Hara et al. [8], our method is able to approximately compute the refraction index of the liquid. This explains the good results for oil, which has a refraction index of 1.47, which is very different to the assumed one of 1.33 for the method of Hara et al. [8]. The usage of 1.33 also explains why Hara et al. [8] perform better for water.

2) Distinction between liquids: In this experiment we used the estimated refractiveness from the optimization problem Eq. (22) to distinguish between the liquids. We restrict ourselves first to the classification between clear liquids and later on we show how well we can classify between clear and opaque liquids. For the evaluation we compare two different liquids with their refractiveness, denoted by $\{r_1, r_2\}$, known beforehand. For the classification, we compare looking up the refraction indexes of the liquid to learning the value from training data. For each test run we use all but this run for training and first compute the angle and raw height values $\{D_{h_r}, D_\alpha\}$.

Table III contains the classification rate for the real and trained refraction index values for the five transparent liquids we collected. We use the maximum value of Eq. (22) optimized over the refractive indices $\{r_1, r_2\}$ instead of the whole range $[n_L, n_H] \cup \{\infty\}$ to classify the unknown liquid.

TABLE II

FLUID LEVEL ERROR IN %

Height	25 %		50 %	
Liq. \ Meth.	HARA14	RGB_DEPTH	HARA14	RGB_DEPTH
Water	9.6 ± 5.1	9.7 ± 11.0	6.2 ± 6.0	2.9 ± 3.9
Vodka	9.4 ± 4.0	4.9 ± 5.5	13.7 ± 2.8	9.0 ± 10.6
Olive Oil	16.5 ± 3.8	6.0 ± 4.6	23.4 ± 6.9	14.0 ± 3.2
Cola	19.8 ± 1.2	6.3 ± 5.9	22.2 ± 0.7	7.5 ± 4.6
Apple juice	18.6 ± 2.3	7.2 ± 5.8	20.3 ± 0.9	2.9 ± 2.2
Orange juice	62.1 ± 2.2	60 ± 1.7	67.6 ± 0.1	5.7 ± 1.1
Milk	67.6 ± 2.8	52.8 ± 2.6	65.9 ± 1.1	4.1 ± 2.4
Height	75 %		100 %	
Water	4.6 ± 4.4	5.3 ± 2.4	4.7 ± 4.9	10.9 ± 5.5
Vodka	6.2 ± 5.0	6.6 ± 11.6	9.6 ± 22.9	8.8 ± 21.3
Olive Oil	20.3 ± 6.4	4.7 ± 3.1	16.7 ± 0.9	3.3 ± 3.4
Cola	1.9 ± 0.9	8.9 ± 5.8	4.5 ± 1.0	14.3 ± 1.0
Apple juice	2.5 ± 0.7	1.8 ± 1.5	12.3 ± 2.0	3.5 ± 2.9
Orange juice	41.5 ± 1.1	1.9 ± 2.0	16.7 ± 0.9	0.9 ± 1.1
Milk	41.2 ± 1.0	1.6 ± 1.8	16.4 ± 0.8	1.0 ± 0.9

TABLE III

CLASSIFICATION RATE IN %

real n \ trained n	Water	Vodka	Olive Oil	Cola	Apple Juice
Water	-	54.28	61.36	**76.47**	85.29
Vodka	45.71	-	**80.00**	80.00	80.00
Olive Oil	68.18	**80.00**	-	94.12	**82.35**
Cola	32.35	**84.00**	**94.12**	-	**79.17**
Apple Juice	50.00	60.00	**67.65**	50.00	-

The bold values denote the classification results, which are statistically significantly better than random guesses under the significance level of 5 %. The refraction index of olive oil, i.e., 1.47, differs from the four other clear liquids, which have a refraction index in the range of $[1.33, 1.37]$. This explains the better classification results for olive oil. Opaque liquids like milk and orange juice do not act like refractive material under the Kinect, but rather like materials with an infinite refractive index. For the comparison between transparent and opaque liquids we use the refractiveness given by the optimization problem Eq. (22) and classify a liquid as opaque if its refractiveness is ∞. In Table IV one can see the classification rates between opaque and transparent liquids for different filling levels. For all heights we obtain classification results, which are statistically significantly better than random guesses under the significance level of 1 %.

V. CONCLUSION AND FUTURE WORK

We presented a novel probabilistic model for determining the heights of liquids in a cup based on data obtained from a widely available RBG-D camera. The model combines information from both RGB and depth data for liquid height detection. Our model works without prior knowledge of the liquid's physical properties like its opaqueness or its refraction index. In fact, our method is able to distinguish between opaque and transparent liquids. With this model, domestic service robots will be able to determine if a cup is empty or partially filled. This is important for tasks such as pouring and determining constraints when picking up and transporting a cup. For future work, we are looking at extending our models to transparent containers such as a glass cup.

TABLE IV

OPAQUE VS. TRANSPARENT LIQUID

Fluid Level	Classification rate in %
25 %	**68.97**
50 %	**73.21**
75 %	**97.59**
100 %	**94.29**
All heights	**86.42**

REFERENCES

[1] M. R. Andersen, T. Jensen, P. Lisouski, A. K. Mortensen, M. K. Hansen, T. Gregersen, and P. Ahrendt. Kinect depth sensor evaluation for computer vision applications. Thechnical report ECE-TR-6, Department of Engineering, Aarhus University, 2012.

[2] R. Bhattacharyya, C. Florkemeier, and S. Sarma. RFID tag antenna based sensing: Does your beverage glass need a refill? In *Proc. of the IEEE Int. Conf. RFID*, 2010.

[3] S. Chitta, J. Sturm, M. Piccoli, and W. Burgard. Tactile sensing for mobile manipulation. *IEEE Transactions on Robotics*, 27(3):558–568, 2011.

[4] P. H. Dietz, D. Leigh, and W. S. Yerazunis. Wireless liquid level sensing for restaurant applications. In *Proc. of the IEEE Int. Conf. on Sensors*, 2002.

[5] C. Elbrechter, J. Maycock, R. Haschke, and H. Ritter. Discriminating liquids using a robotic kitchen assistant. In *Proc. of the IEEE/RSJ Int. Conf. on Intelligent Robots and Systems (IROS)*, 2015.

[6] M. A. Fischler and R. C. Bolles. Random sample consensus: A paradigm for model fitting with applications to image analysis and automated cartography. *Communications of the ACM*, 24(6):381–395, 1981.

[7] H.-W. Gellersen, M. Beigl, and H. Krull. The mediacup: Awareness technology embedded in an everyday object. In *Handheld and Ubiquitous Computing*, pages 308–310. Springer, 1999.

[8] Y. Hara, F. Honda, T. Tsubouchi, and A. Ohya. Detection of liquids in cups based on the refraction of light with a depth camera using triangulation. In *Proc. of the IEEE/RSJ Int. Conf. on Intelligent Robots and Systems (IROS)*, 2014.

[9] U. Klank, D. Carton, and M. Beetz. Transparent object detection and reconstruction on a mobile platform. In *Proc. of the IEEE Int. Conf. on Robotics & Automation (ICRA)*, 2011.

[10] I. Lysenkov, V. Eruhimov, and G. Bradski. Recognition and pose estimation of rigid transparent objects with a kinect sensor. In *Proc. of Robotics: Science and Systems (RSS)*, 2012.

[11] N. J. Morris and K. N. Kutulakos. Dynamic refraction stereo. *IEEE Transactions on Pattern Analysis and Machine Intelligence*, 33(8): 1518–1531, 2011.

[12] K. J. Pithadiya, C. K. Modi, and J. D. Chauhan. Selecting the most favourable edge detection technique for liquid level inspection in bottles. *Int. Journal of Computer Information Systems and Industrial Management Applications (IJCISIM) ISSN*, pages 2150–7988, 2011.

[13] G. Schwarz et al. Estimating the dimension of a model. *The annals of statistics*, 6(2):461–464, 1978.

[14] T. Wang, X. He, and N. Barnes. Glass object localization by joint inference of boundary and depth. In *21st Int. Conf. on Pattern Recognition (ICPR)*, pages 3783–3786. IEEE, 2012.